

See discussions, stats, and author profiles for this publication at: <https://www.researchgate.net/publication/231679080>

X-ray Diffraction of Photonic Colloidal Single Crystals

ARTICLE *in* LANGMUIR · NOVEMBER 1997

Impact Factor: 4.46 · DOI: 10.1021/la970423n

CITATIONS

103

READS

83

4 AUTHORS:



Willem L. Vos

University of Twente

223 PUBLICATIONS 6,639 CITATIONS

SEE PROFILE



Mischa Megens

Philips

54 PUBLICATIONS 1,862 CITATIONS

SEE PROFILE



Carlos van kats

Utrecht University

27 PUBLICATIONS 1,086 CITATIONS

SEE PROFILE



Peter Boesecke

European Synchrotron Radiation Facility

32 PUBLICATIONS 956 CITATIONS

SEE PROFILE

X-ray Diffraction of Photonic Colloidal Single Crystals

Willem L. Vos,^{*,†} Mischa Megens,[†] Carlos M. van Kats,^{†,‡} and Peter Bösecke^{§,||}

van der Waals-Zeeman Instituut, Universiteit van Amsterdam,
NL-1018 XE Amsterdam, The Netherlands, and European Synchrotron Radiation Facility,
BP 220, F-38043 Grenoble Cédex, France

Received April 24, 1997. In Final Form: June 16, 1997[®]

We have resolved a great number of Bragg peaks of photonic colloidal *single* crystals by synchrotron small angle X-ray scattering (SAXS). We find that charge-stabilized colloids form face-centered cubic crystals at all densities up to ~60 vol %. The colloidal particles are highly ordered on their lattice sites, which confirms that these self-organizing materials are suitable building blocks for optical photonic matter. The experiments demonstrate that synchrotron SAXS with two-dimensional detection is a powerful tool to study systems with length scales comparable to optical wavelengths.

An attractive feature of colloidal suspensions¹ is the ability to spontaneously form bulk three-dimensional (3D) crystals with lattice parameters on the order of 1–1000 nm.² It is thus natural to consider colloidal crystals as nanostructured materials,³ in particular as photonic crystals.⁴ Photonic crystals are three-dimensional dielectric structures with lattice parameters comparable to the wavelength of light, that influence the propagation of photons in the same way that atomic crystals determine electronic properties.^{5,6} Photonic crystals are being pursued to obtain a range of forbidden frequencies, called a photonic band gap, that is expected to lead to innovations in optics and quantum optics.^{5–7} Since optical properties are intimately connected to the crystal structure, it is crucial to know the structure of self-organizing photonic colloidal crystals. Strong interaction between photonic crystals and light, however, causes multiple scattering, which hampers structure determination by light scattering or other optical methods.^{8,9} Therefore, we use small angle X-ray scattering (SAXS)¹⁰ with a synchrotron source, which has the advantages of a high wavelength resolution, a tightly focused beam, and a high photon flux, in comparison to e.g. neutron scattering. We observe large numbers of Bragg diffraction peaks of photonic colloidal *single* crystals over an unprecedented range of scattering vectors. The colloidal particles order in face-centered cubic

(fcc) structures at all densities and with a high degree of localization about their lattice sites. This is an excellent starting point for photonic band gap crystals,¹¹ as opposed to disordered structures that have been observed before.^{12,13}

Charge-stabilized colloids are an important class of colloids² that are particularly promising for photonic purposes, because the lattice parameters can be tuned with the ionic strength.¹ The photonic properties are optimal for particle densities ϕ in the range 20–50 vol %, because the Bragg resonances of the lattice are then matched with the internal Mie resonances of the particles.^{4,15,16} The crystal structure of dense charge-stabilized colloids with $\phi > 10$ vol % is expected to be fcc.² Interestingly however, experiments at $\phi > 30$ vol % have revealed glass formation instead of crystallization.¹² Application of shear prevents vitrification but results in random stacks of hexagonal close-packed planes (rhcp)¹³ or possibly hexagonal close packing (hcp)¹⁴ instead of fcc packing. We find that our samples do form photonic fcc crystals over a wide range of densities, which confirms the original notion.² The practical usefulness of photonic colloidal crystals also depends on the availability of sufficiently large single crystals. Indeed crystals with linear dimensions on the order of 10^4 unit cells (mm sizes) have been reported, albeit for dilute, weakly photonic samples with $\phi < 1$ vol %.^{17,18} The largest crystals are grown close to the freezing curve, where the nucleation rate is so small that few crystal grains nucleate and grow (cf. Figure 1).¹⁹ Dense crystals with $\phi \sim 50$ vol % have been made with sterically stabilized colloids, but the crystallites are smaller with linear dimensions of 20–100 μm .² We have grown charge-stabilized single crystals with volume fractions up to 60 vol % and dimensions up to 0.5

* To whom correspondence should be addressed. E-mail: wvos@phys.uva.nl, <http://gopher.phys.uva.nl:70/0/fnsis/onderzoek/scm/scmhome.htm>.

[†] Universiteit van Amsterdam.

[‡] Present address: van't Hoff Laboratorium, Universiteit Utrecht, NL-3584 CH Utrecht, The Netherlands.

[§] European Synchrotron Radiation Facility.

^{||} Present address: MPG/ASMB c/o DESY, Notkestrasse 85, D-22603 Hamburg, Germany.

[®] Abstract published in *Advance ACS Abstracts*, October 1, 1997.

(1) Hunter, R. J. *Foundations of Colloid Science*; Clarendon: Oxford, 1992.

(2) Pusey, P. N. In *Liquids, Freezing, and Glass Transition*; Levesque, D., Hansen, J.-P., Zinn-Justin, J., Eds.; Elsevier: Amsterdam, 1991; p 763. Poon, W. C. K.; Pusey, P. N.; Lekkerkerker, H. N. W. *Phys. World* **1996**, 9, 27.

(3) Siegel, R. W. *Phys. Today* **1993**, 46 (10), 64.

(4) John, S. *Phys. Today* **1991**, 44 (5), 32.

(5) Yablonovitch, E. *Phys. Rev. Lett.* **1987**, 58, 2059. John, S. *Phys. Rev. Lett.* **1987**, 58, 2486.

(6) Bowden, C. M.; Dowling, J. P.; Everitt, H. O., Eds. Development and applications of materials exhibiting photonic band gaps. *J. Opt. Soc. Am. B* **1993**, 10, 280.

(7) Gourley, P. L. *Nature* **1994**, 371, 571.

(8) Vos, W. L.; Sprik, R.; van Blaaderen, A.; Imhof, A.; Lagendijk, A.; Wegdam, G. H. *Phys. Rev. B* **1996**, 53, 16231; **1997**, 55, 1903(E).

(9) Vos, W. L.; Sprik, R.; Lagendijk, A.; Wegdam, G. H.; van Blaaderen, A.; Imhof, A. In *Photonic Band Gap Materials*; Sukoulis, C. M., Ed.; Kluwer: Dordrecht, 1996; p 107.

(10) Feigin, L. A.; Svergun, D. I. *Structure Analysis by Small-Angle X-ray and Neutron Scattering*; Plenum: New York, 1987.

(11) Sözüer, H. S.; Haus, J. W.; Inguva, R. *Phys. Rev. B* **1992**, 45, 13962.

(12) Sirota, E. B.; Ou-Yang, H. D.; Sinha, S. K.; Chaikin, P. M.; Axe, J. D.; Fujii, Y. *Phys. Rev. Lett.* **1989**, 62, 1524.

(13) Ackerson, B. J.; Hayter, J. B.; Clark, N. A.; Cotter, L. *J. Chem. Phys.* **1986**, 84, 2344. Versmold, H.; Lindner, P. *Langmuir* **1994**, 10, 3043. Dux, C.; Versmold, H.; Reus, V.; Zemb, T.; Lindner, P. *J. Chem. Phys.* **1996**, 104, 6369.

(14) Clarke, S. M.; Rennie, A. R.; Ottewill, R. H. *Langmuir* **1997**, 13, 1964.

(15) Yablonovitch, E.; Gmitter, T. J. *Phys. Rev. Lett.* **1989**, 63, 1950.

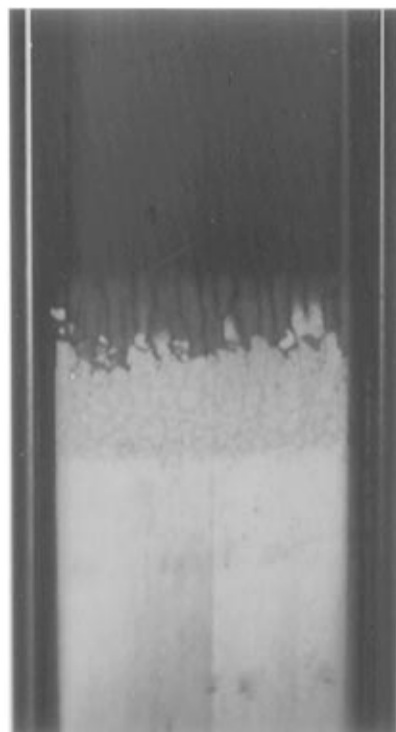
(16) Vos, W. L.; Megens, M.; van Kats, C. M.; Bösecke, P. *J. Phys.: Condens. Matter* **1996**, 8, 9503.

(17) Okubo, T. *Langmuir* **1994**, 10, 1695.

(18) Palberg, T.; Mönch, W.; Schwarz, J.; Leiderer, P. *J. Chem. Phys.* **1995**, 102, 5082.

(19) Kelton, K. F. In *Solid State Physics*; Ehrenreich, H.; Turnbull, D., Eds.; Academic: New York, 1991; p 75. Brugmans, M. J. P.; Vos, W. L. *J. Chem. Phys.* **1995**, 103, 2661.

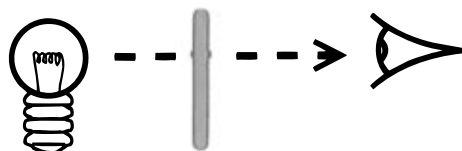
Transmission



liquid

crystals

powder



Reflection

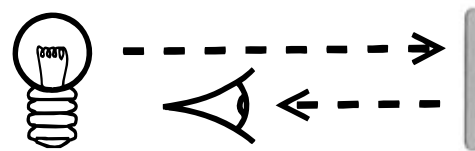


Figure 1. Photographs of a photonic colloidal sample of sedimented polystyrene spheres (radii, 100.9 nm; size polydispersity, 2.3 nm) in methanol, contained in a 4 mm wide capillary. The pictures were taken with white light, in transmission (left) and in reflection (right) modes, as indicated by the cartoons. For a comparison of the images, some light was also reflected in the left picture. The density of colloids increases from top to bottom. In the upper part of the sample, the particles form a colloidal liquid in which incident light is randomly multiple scattered; hence, it appears opaque in transmission mode and white in reflection mode. In contrast, photonic crystals transmit incident light unless Bragg reflections occur, which are a precursor of photonic band gaps.^{5,6} In this particular sample, green light is Bragg reflected (right panel) and the red part of the optical spectrum is transmitted (left panel). The green Bragg reflections are caused by close-packed crystal planes parallel to the capillary wall (fcc 111 planes). Just below the liquid, crystals are visible that are large enough for a single-crystal diffraction study. They are separated by dark grain boundaries, and several of them are not oriented with the close-packed planes parallel to the glass. Further, below, the sample is polycrystalline ("powder").

mm (see Figure 1), which is large enough to isolate a single photonic crystal for experimental study.

We have studied samples made of polystyrene spheres (Duke Scientific) in water or methanol, that were sealed in 0.3 or 0.4 mm thick flat glass capillaries (Vitro Dynamics). Crystals with densities below 50 vol % were made by deionizing the suspensions with ion exchange resin (BioRad AG501-X8) before the suspension was introduced into the capillaries. The best results were obtained with crystals that nucleated and grew over periods on the order of months. Addition of extra ion resin to the capillaries increased the nucleation and growth rates, which resulted in more and smaller crystals. Dense crystals ($\phi > 50$ vol %) were grown by sedimentation of charge-screened colloids at accelerations of ~ 400 g. This corresponds to a ratio of the sedimentation velocity to diffusion velocity (known as the Peclet number) of about 0.02, which suggests that the sediment is in thermodynamic equilibrium. The crystal-liquid interface appears at densities near 50 vol %, close to the hard sphere crystallization density. After ~ 4 h, relatively large grains develop at the crystal-liquid interface, that anneal to

sizes on the order of 0.5 mm. Longer centrifugation times result in compression of the crystals ($\phi > 60$ vol %), but also cause them to break up into a polycrystalline assembly.²⁰

The SAXS experiments were performed on beamline 4 of the European Synchrotron Radiation Facility (ESRF).²¹ The incident beam was monochromatic with a wavelength $\lambda = 0.09880$ nm and a bandwidth $\Delta\lambda/\lambda = 1.5 \times 10^{-4}$. It was focused to a narrow spot of about $0.2 \text{ mm} \times 0.5 \text{ mm}$, with a maximum beam flux of 10^{13} photons/s. The scattered radiation was detected with a two-dimensional gas-filled detector at the maximum distance of 10 m from the sample. This has the advantage over other SAXS cameras that the scattering pattern is not smeared and that no scanning is necessary.²² The smallest scattering vector $s = 2 \sin(\theta)/\lambda$, with θ the diffraction angle, is 0.002 nm^{-1} . The resolving power is $\Delta s \sim 7 \times 10^{-4} \text{ nm}^{-1}$ in both

(20) Megens, M.; van Kats, C. M.; Bösecke, P.; Vos, W. L. *Proceedings X International Conference on Small Angle Scattering*, Craievich, A., Teixeira, J., Kistorz, G., Eds.; *J. Appl. Crystallogr.*, in press.

(21) Bösecke, P.; Diat, O.; Rasmussen, B. *Rev. Sci. Instrum.* **1995**, *66*, 1636.

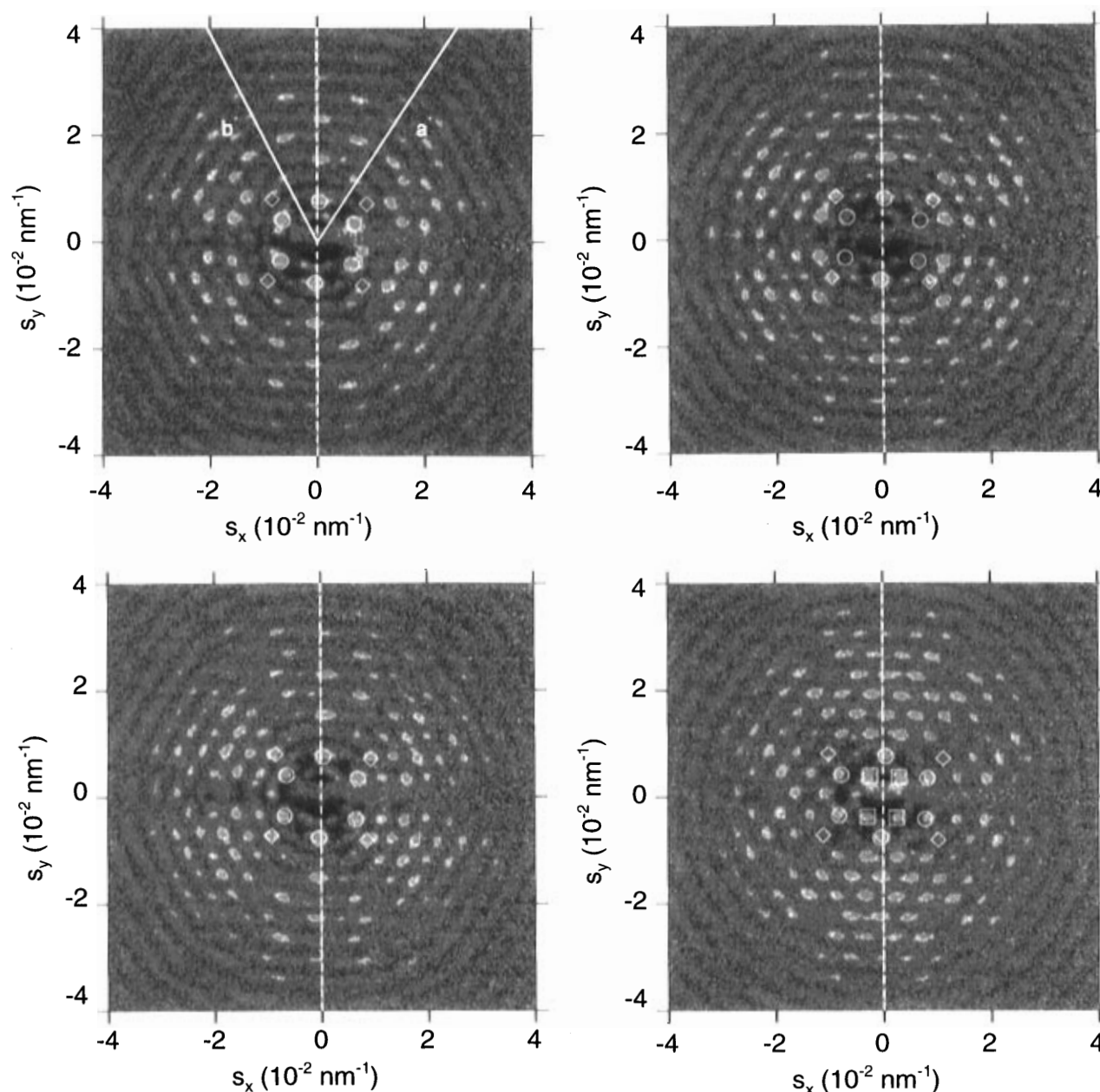


Figure 2. Structure factors at several angles of incidence ω of a colloidal single crystal of $r = 120.8$ nm polystyrene spheres (size polydispersity, 1.6 nm) in water with a volume fraction $\phi = 56$ vol %: (A, top left) data for $\omega = 0^\circ$; (B, top right) data for $\omega = 6^\circ$; (C, bottom left) data for $\omega = 14^\circ$; (D, bottom right) data for $\omega = 34^\circ$. The drawn lines are the a^* and b^* axes in reciprocal space. The rotation axis is $s_x = 0$ (dashed lines); hence, the spots on this axis are unchanged. The circles indicate the six $hk = 11$ class Bragg rods, which peak at $l = 0$ (panel A), and $l = 1$ (panel D). The diamonds indicate the $hk = 31$ Bragg rods, which peak at $l = 1/3$ (panel B). The squares in panel D indicate the peaks on the $hk = 10$ Bragg rods, that appear at $\omega = 34^\circ$. These four reflections correspond to the close-packed reflections of fcc packing ($hkl_{\text{fcc}} = 111$). The patterns have been collected for 105 s; they have been corrected for the detector response and for the single-particle form factor, that was measured separately.^{20,29}

dimensions.²¹ The capillaries were mounted with their long axis vertical on two translation stages that scanned the spatial position with respect to the horizontal X-ray beam, and a rotation stage that scanned about the long axis of each sample (ω -axis).²³

Figure 2 presents X-ray scattering patterns of a single crystal consisting of $r = 120.8$ nm spheres with a lattice parameter $a = 370$ nm and a volume fraction $\phi = 56$ vol %. Many Bragg peaks are seen, which indicates that the spheres are ordered in a crystalline array. If the sample

is translated, we observe doubling or tripling of each peak or even concentric rings at the radii of the peaks, which means that the incident beam then irradiates two, three, or many crystals, respectively. Therefore, Figure 2 shows indeed the scattering patterns of a single colloidal crystal. Many Bragg diffraction peaks are observed simultaneously, in contrast to X-ray diffraction of atomic single crystals.²³ The reason is that the wavelength λ is much smaller than the typical lattice spacings d ; hence, the radius $1/\lambda$ of the Ewald scattering sphere²³ is much larger than the lengths $1/d$ of the reciprocal lattice vectors. Consequently, the Ewald sphere becomes a scattering plane that simultaneously intersects many reciprocal lattice vectors.^{13,23} The Bragg peaks in Figure 2A have approximately a sixfold symmetry. This is expected

(22) Bonse, U.; Hart, M. *Appl. Phys. Lett.* **1965**, *7*, 238. Doshio, S.; Ise, N.; Ito, K.; Iwai, S.; Kitano, H.; Matsuoka, H.; Nakamura, H.; Okomura, H.; Ono, T.; Sogami, I. S.; Ueno, Y.; Yoshida, H.; Yoshiyama, T. *Langmuir* **1993**, *9*, 394. Diat, O.; Bösecke, P.; Ferrero, C.; Freund, A. K.; Lambard, J.; Heintzmann, R. *Nucl. Instrum. Methods A* **1995**, *356*, 566.

(23) Guinier, A. *X-ray Diffraction*; Freeman: San Francisco, CA, 1963.

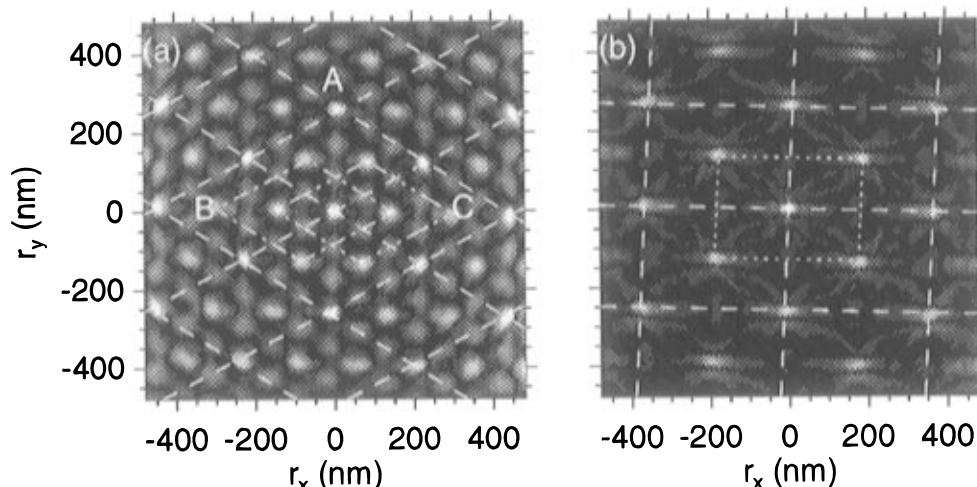


Figure 3. Real space density autocorrelation functions (Patterson maps). (a, left) Cubic 111 planes ($\omega = 0$ in Figure 2A). The hexagonal unit cell with edge lengths equal to the nearest neighbor distance of ~ 260 nm is indicated with dashed lines. The dashed-dotted cell indicated with "B" and the dashed-triple-dotted cell indicated with "C" are hexagonal units in planes just above or just below the central "A" plane. (b, right) Cubic 110 planes ($\omega = 34^\circ$ in Figure 2B). The dashed grid indicates the projected square faces of the cubic unit cell, with edges equal to 260 nm and to $\sqrt{2} \times 260$ nm. The dotted rectangle indicates the correlations due to planes above and below the one indicated with dashed lines. The data have been corrected for the profile of the direct beam and the detector response function.

because dense colloids usually order in hexagonal close-packed planes that lie parallel to cell windows.² The stacking sequence of these planes determines whether the structure is fcc, hcp, random stacking, or a complex sequence (e.g. double or triple hcp).²³ Therefore, the reciprocal space consists of a hexagonal arrangement of Bragg rods, labeled with Miller indices h , k , and an index l indicating the distance along the rods.²³ In normal incidence (Figure 2A), $l = 0$ and we are looking down the c -axis. The inner six Bragg peaks in Figure 2A are the $hk = 11$ class reflections. These peaks cannot be the $hk = 10$ class, because this would result in an unphysical density beyond close packing of $\phi = 88$ vol %. The absence of $hk = 10$ indicates that the crystal is fcc, on the basis of considerations of intensity distributions on the Bragg rods.²³ In Figure 2A, most bright and dark spots occur under conditions expected for fcc packing namely $h - k = 3n$ and $h - k = 3n \pm 1$, respectively.

In order to sweep the third dimension of reciprocal space, the scattered intensity was measured as a function of the angle of incidence ω (Figure 2A-D). Intersections of the Ewald scattering plane with reciprocal lattice vectors are seen as Bragg spots on the detector, that appear and disappear upon rotation.²⁴ As a visual aid, we have indicated the positions of several classes of Bragg rods in Figure 2A-D. It is clearly seen that with increasing angle, the $hk = 11$ spots (circles) become weaker (B), completely disappear (C), and reappear at $\omega = 34^\circ$ (panel D). The $hk = 31$ spots (diamonds), on the other hand, start with zero intensity in panel A, have a maximum at 6° (panel B), become weaker (panel C), and have completely disappeared in panel D. The maxima for the 11 class correspond to $l = 0$, and $l = 1$ respectively, which confirms that the crystal consists of interlocked stacks of hexagonal planes.^{13,23} The maximum intensities for $hk = 31$ appear at $l = 1/3$, which confirms that the crystal structure is untwinned fcc, and not any other stacking of hexagonal planes such as hcp or rhcp.²³ Moreover, at $\omega = 34^\circ$ (Figure 2D), four spots have appeared close to the beam stop, closer than the $hk = 11$ class reflections (squares). They are the

$hk = 10$ class with $l = 1/3$, that correspond to the cubic 111 reflections of the close-packed planes, whereas these reflections are absent in hexagonal structures. The 111 reflections perpendicular to the capillary wall are the ones that are visually observed in Figure 1, which demonstrates that SAXS resolves length scales on the order of optical wavelengths. The Bragg peaks shown in Figure 2 can be azimuthally averaged to obtain a pattern as a function of the diffraction angle, similar to patterns of polycrystalline samples. It turns out that the Bragg diffraction angles are very well explained with fcc lattice spacings. This confirms our observation of fcc diffraction patterns in polycrystalline samples of charge-stabilized spheres.²⁰ We take the observation of fcc packing at densities over the range 20–60 vol % as evidence that this is indeed the stable phase of dense charge-stabilized colloids,² in contrast to rhcp or glass. The observation of the fcc structure has important consequences for photonics:²⁵ this structure excludes a larger portion of the density of radiating optical states in the close-packed directions compared to the case of disordered structures, which results in a larger quantum optical modification of the spontaneous emission rate.

An important feature in the diffraction patterns is the large number of diffraction peaks up to large scattering vectors (Figure 2). This indicates that the Debye–Waller factor is small, which means that the root-mean-square excursions u_{rms} of the colloidal spheres from their ideal crystal positions are small.²³ For the patterns in Figure 2, we find a u_{rms} of only 3.5% of the nearest neighbor distance. Bragg peaks correspond to lattice vectors in reciprocal space, that play a central role in band structure calculations of the propagation of light through photonic crystals.⁶ Thus a high degree of order is crucial for photonic crystals, because the observation of a large number of reciprocal lattice vectors means that the optical band structures are well defined up to high optical frequencies.⁶ A more elaborate analysis is in progress, because Debye–Waller factors of colloidal crystals may

(24) The patterns observed as a function of angle of incidence (Figure 2) are best viewed on the movie animation which is available as Supporting Information on the World Wide Web or through the authors.

(25) Sprik, R.; van Tiggelen, B. A.; Lagendijk, A. *Europhys. Lett.* **1996**, *35*, 265.

provide constraints on the interactions in dense colloids, which are currently subject to debate.²⁶

The basic goal of a diffraction study is to obtain a real space image of the positions of particles in a crystal. Whereas direct imaging is hampered by the well-known phase problem in diffraction,²³ one can already obtain much insight from Fourier transforms of the diffraction patterns. In parts a and b of Figure 3, we have plotted the Fourier transforms of Figure 2A and D, respectively. This yields projections of the auto-correlation function of the density in real space, which is a map of the vectors that connect particle positions, known as the Patterson map.²³ These maps are especially useful to elucidate complex structures of non-overlapping particles, typical of colloidal systems. Figure 3a shows the Patterson function projected on a plane perpendicular to the cubic 111 axis. The dashed lines indicate the hexagonal close-packed plane ('A' in Figure 3a). The clear spots on the corners of each cell indicate the distance to nearest neighbors and next nearest neighbors in the hexagonal planes. The spots should not be confused with the real space density obtained in a hologram or a microscope image. It is well-known that the fcc structure can be represented as a three-layer repeat sequence ABCABC... of hexagonal close-packed layers;²³ thus, there are two other planes that are located below and above an 'A' plane. In Figure 3a, these give rise to additional peaks, that are indicated with 'B' and 'C'. Additional correlations at positions in between the ideal lattice points are possibly caused by defects in the crystal. Figure 3b shows the Patterson function projected perpendicular to a cubic 110 axis. We have indicated the rectangular pattern with edge ratio $1:\sqrt{2}$ times the nearest neighbor distance of ~ 260 nm. The cubic 110 direction is vertical (as in Figure 3a), and the cubic 100 direction is now horizontal. The midpoints in the rectangles are caused by particles in planes below and above a particular 110 plane, that are displaced by one nearest neighbor distance. The orientation of the unit cell is such that one cubic 110 axis is pointing upward, which means that rows of particles in the close-packed planes are parallel to the sedimentation

direction. Such an orientation is usually observed in sheared samples¹³ but does not always occur in our samples (cf. Figure 1). The range in real space of the Patterson functions is currently limited to about 500 nm by the shape of the incident beam and the detector response function. The extension to the micron range is anticipated.

The growth and observation of highly ordered fcc crystals strongly support the notion that self-organizing soft condensed matter is a suitable building block for photonic matter. It is thus exciting that there are novel developments to control the growth of colloidal crystals.²⁷ Moreover, crystals with structures of interest to photonic applications have recently been found in binary mixtures.²⁸ Our results demonstrate that synchrotron SAXS with two-dimensional detection (Figure 2) is a powerful technique to investigate systems with length scales on the order of optical wavelengths, especially when they are strongly photonic,^{8,9,16} in other words strongly multiple scattering.

Acknowledgment. We thank Ad Lagendijk, Gerard Wegdam, Rudolf Sprik, and Alfons van Blaaderen for encouragement and the staff of ESRF for help. This work is part of the research programme of the 'Stichting voor Fundamenteel Onderzoek der Materie (FOM)', which is financially supported by the 'Nederlandse Organisatie voor Wetenschappelijk Onderzoek (NWO)'.

Supporting Information Available: Electronic file containing the data shown in Figure 2 that is available via the World Wide Web. See any current masthead page for access information.

LA970423N

(27) Burns, M. M.; Fournier, J. M.; Golovchenko, J. A. *Science* **1990**, *249*, 749. Zhu, J. X.; Chaikin, P. M.; Li, M.; Russell, W. B.; Meyer, W. V.; Rogers, R. B. *OSA Conference "Photon Correlation and Scattering"*, Capri, Italy, August 21–24, 1996; van Blaaderen, A.; Ruel, R.; Wiltzius, P. *Nature* **1997**, *385*, 321.

(28) Bartlett, P.; Ottewill, R. H.; Pusey, P. N. *Phys. Rev. Lett.* **1992**, *68*, 3801. Vos, W. L.; Finger, L. W.; Hemley, R. J.; Hu, J. Z.; Mao, H.-k.; Schouten, J. A. *Nature* **1992**, *358*, 46.

(29) Dingenouts, N.; Kim, Y. S.; Ballauf, M. *Colloid Polym. Sci.* **1994**, *272*, 1380. Megens, M.; van Kats, C. M.; Bösecke, P.; Vos, W. L. *Langmuir* **1997**, *13*, 6120.

(26) Larsen, A. E.; Grier, D. G. *Nature* **1997**, *385*, 230.